

Splitting of reinforced concrete panels under concentrated loads

Stephen J. Foster†

School of Civil and Environmental Engineering, The University of New South Wales, Sydney, 2052, Australia

David M. Rogowsky‡

Department of Civil and Environmental Engineering, University of Alberta, Edmonton, T6G 2G7, Canada

Abstract. It is well understood that concentrated forces applied in the plane of a beam or panel (such as a wall or slab) lead to splitting forces developing within a disturbed region forming beyond the bearing zone. In a linearly elastic material the length of the disturbed region is approximately equal to the depth of the member. In concrete structures, however, the length of the disturbed region is a function of the orthotropic properties of the concrete-steel composite. In the detailing of steel reinforcement within the disturbed regions two limit states must be satisfied; strength and serviceability (in this case the serviceability requirement being acceptable crack widths). If the design requires large redistribution of stresses, the member may perform poorly at service and/or overload. In this paper the results of a plane stress finite element investigation of concentrated loads on reinforced concrete panels are presented. Two cases are examined (i) panels loaded concentrically, and (ii) panels loaded eccentrically. The numerical investigation suggests that the bursting force distribution is substantially different from that calculated using elastic design methods currently used in some codes of practice. The optimum solution for a uniformly reinforced bursting region was found to be with the reinforcement distributed from approximately 0.2 times the effective depth of the member ($0.2D_e$) to between $1.2D_e$ and $1.6D_e$. Strut and tie models based on the finite element analyses are proposed herein.

Key words: strut and tie; splitting; bursting; disturbed regions.

1. Introduction

Disturbed zones in concrete structures represent complex regions where the assumption that plane sections remain plane (the Bernoulli hypothesis) does not hold true. In slabs, beams and walls where a concentrated compressive load is applied (for example at a prestressed concrete anchorage) the stress disperses through a transition zone (the St Venant's region) to a plane within the panel where Bernoulli's hypothesis is essentially true. The dispersion of compression stresses through the St. Venant's zone produces transverse tension strain fields. If uncontrolled the transverse tension strains can lead to excessive cracking in the major principal direction and a loss of concrete compressive strength in the minor principal direction (Vecchio and Collins 1986). In the case of normal reinforced concrete structures, steel reinforcement is used to carry

† Ph.D., Senior Lecturer

‡ Ph.D., P. Eng., Professor

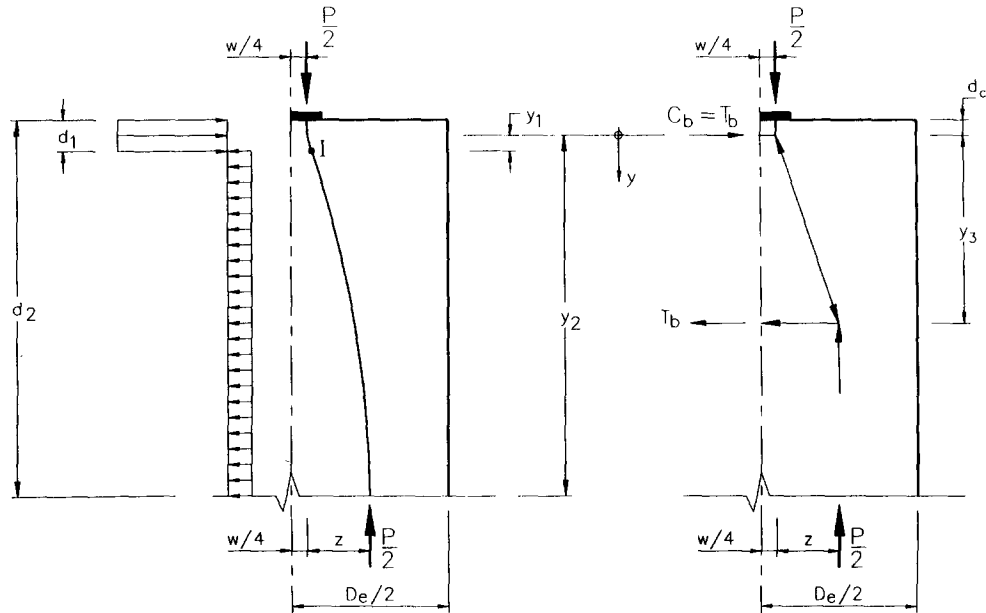


Fig. 1 Parabolic stress distribution of Mörsch (1924) with the statically equivalent strut and tie model.

these tension forces and to control cracking.

A popular method for the design of the disturbed regions is to develop a suitable strut and tie model. The strut and tie model, however, should not vary greatly from the “natural” behaviour of the steel-concrete composite panel unless it can be shown that the panel has sufficient ductility to redistribute the internal forces. In this context “natural” being the way the panels “want to behave” without being excessively pushed. If the panel behaviour is governed by the reinforcing steel (a primary tension failure), significant redistribution can be achieved. However, if the panel fails in a primary compression mode little redistribution is possible. In the case of compression failures in deep beams, for example, little - if any - internal force redistribution can be expected unless heavy web reinforcement is used (Rogowsky and MacGregor 1983, Foster 1992a).

In this study, the behaviour of centrally and eccentrically loaded panels are examined using non-linear finite element (FE) models. The numerical study is aimed at providing guidance on where best to locate the steel reinforcement such that i) bursting failures can be avoided, and ii) to produce an efficient design. While it is recognised that a primary mode of failure is that of bearing, this mode of failure is not investigated in this study.

2. A simple design model

Mörsch (1924) proposed using quadratic stress trajectories to define the compressive stress field through the St. Venant's region of a panel subjected to an in-plane concentrated load. With this assumption the forces transverse to the line of the applied loading are uniformly distributed through the bursting region (as shown for the concentrically loaded panel in Fig. 1). With this model the bursting tension (T_b) is

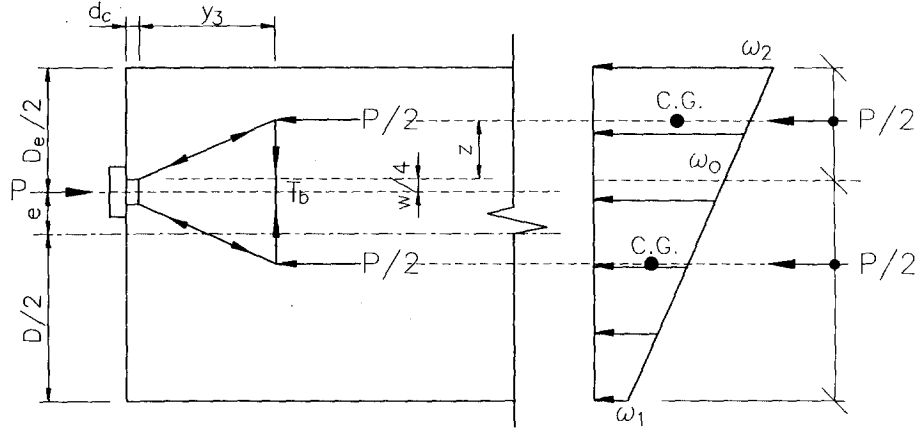


Fig. 2 Strut and tie model for an eccentrically loaded panel.

$$T_b = \frac{Pz}{y_1 + y_2} = \frac{Pz}{d_1 + d_2 - 2d_c} \quad (1)$$

where P is the applied load, z is the distance between line of action of the $1/2$ bearing force to the line of action of its equilibrium force at the junction of the Bernoulli and St. Venant's regions and y_1 , y_2 , d_1 , d_2 and d_c are as shown in Fig. 1. Here the shape of the compression strut is defined by two parabolas, one through the range $-y_1 \leq y \leq y_1$ and a second through the range $y_1 \leq y \leq y_2$.

The model shown in Fig. 1 can be replaced with a statically equivalent, strut and tie model. In the most general form of this model (shown in Fig. 2) the bursting force is given by

$$T_b = \frac{Pz}{2y_3} \quad (2)$$

where z is as shown in Fig. 2 and y_3 as the distance between the bursting compression force (C_b) to the centroid of the bursting tension force. For the special case of a centrally loaded symmetric panel $z = (D - w)/4$ and the bursting force given by Eq. (2) becomes

$$T_b = \frac{D}{8y_3} (1 - w/D) P \quad (3)$$

With $y_3 = D/2$ in Eq. (3) the relationship for the bursting forces derived by Mörsch (1924) is obtained. That is

$$T_b = \frac{P}{4} (1 - w/D) \quad (4)$$

For the serviceability limit state, the area of reinforcement needed to carry bursting tension forces is given by

$$A_{st} = T_b / f_s \quad (5)$$

where f_s is the maximum stress in the reinforcement for serviceability. The reinforcement obtained by Eq. (5) is required to be evenly spaced through the region $2d_c$ to $2y_3$ (d_1 to d_2), measured

from the bearing surface. To ensure that satisfactory serviceability is obtained using the strut and tie model discussed above, the transverse strain distribution under service conditions should be almost uniform in the region of the uniformly distributed bursting reinforcement. A significant departure from a uniform distribution of transverse strains may lead to larger crack widths than envisaged by the designer.

In the strength limit state, the reinforcing steel yields and crack widths are generally not of concern. In this case, a wide range of reinforcing arrangements can be utilised. Assuming that all bursting steel will yield, the area of reinforcing steel required to resist the bursting tensions is

$$A_{st} = \frac{T_b}{\phi f_{yt}} \quad (6)$$

where f_{yt} is the yield strength of the reinforcing steel, ϕ is a strength reduction factor and T_b is calculated from Eq. (2) or Eq. (3) as appropriate.

3. Finite element modelling

In order to study the strut and tie models discussed above, a number of two dimensional plane stress finite element (FE) analyses were undertaken. The FE model (Foster 1992b, Foster, *et al.* 1996) takes into consideration the effects of cracking, crushing and the loss of compressive strength due to transverse tension fields and other biaxial effects. In practice the zone of concrete in front of the bearing plate is usually confined by spirals or orthogonal grids of reinforcement to enhance the bearing capacity of the concrete. A zone of strong concrete is used in the region of the bearing plate to simulate the triaxial effects of the confined concrete within this zone. The authors note that the ultimate loads obtained in the numerical modelling may not reflect the ultimate loads obtained in similar laboratory experiments due to the uncertainty of the bearing capacity. The strong zone reflects the local bearing capacity obtained from the experimental studies of others and it is believed that suitable confining reinforcement can be placed to give the loads obtained. This however is not important as the aim of this study is to compare the transverse strain distributions after significant cracking has occurred in the concrete to the elastic stress distributions adopted in earlier studies. Further, there are any number of strut and tie models that give theoretically satisfactory solutions. Numerical experiments have been undertaken to assist one to identify models that produce acceptable results.

3.1. Material modelling

The steel reinforcement is modelled using a three node parabolic element, with two Gauss point integration being used to generate the element stiffness matrix. A bi-linear stress versus strain relationship is used (see Fig. 3a) to model the reinforcing steel with perfect bond being assumed between the steel and the concrete. For all analyses undertaken as a part of this study the yield stress of the reinforcing bar was taken as $f_{yt} = 400 \text{ MPa}$ with an initial elastic modulus of $E_o = 2 \times 10^5 \text{ MPa}$ and a post yield modulus of $E_w = 0.0$.

The stress versus strain model for the plain concrete elements is shown in Fig. 3b. The concrete is modelled using eight node isoparametric plane stress elements with a 3×3 Gauss quadrature

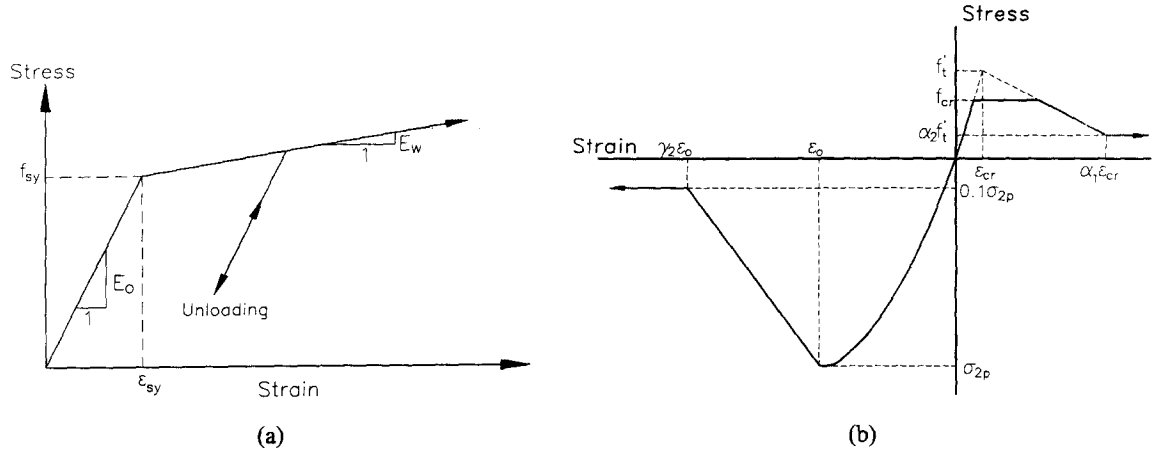


Fig. 3 (a) Stress versus strain relationship for reinforcing steel elements, (b) Uniaxial stress versus strain relationship for plain concrete.

being used to formulate the element stiffness matrix. The element can be in any of four states at any point in the analysis; undamaged, cracked, crushed, or both cracked and crushed.

The undamaged concrete element is formulated using the principle of equivalent uniaxial strains as outlined by Darwin and Pecknold (1977) with modifications to enable the use of a rotating crack model (Foster 1992b, Foster, *et al.* 1996). The family of stress-strain curves selected for compressive loading are those suggested by Saenz (1964), and used by Darwin and Pecknold.

For tension loading the stress versus strain relationship is assumed to be linear with the tangent and secant modulus equal to the initial modulus, E_0 , until the stress reaches the limiting stress defined by the biaxial strength relationship (see Foster, *et al.* 1992b). After cracking a series of linear models are used to describe the tensile strength, as shown in Fig. 3b.

When the biaxial strength criteria is reached then the concrete element undergoes a state of change. If the concrete is in biaxial tension-compression then the concrete cracks perpendicular to the major principal axis. When this occurs the finite element model formulations change to those derived by Vecchio and Collins (1986), with some minor variations on the tension side of the stress-strain graph. The modified compression field theory was developed by Vecchio and Collins to predict the load-deformation response of reinforced concrete elements subjected to in-plane shear and normal stresses, with cracked concrete being treated as a new and different material from its undamaged state.

The concrete strength used in this study was $f'_c = 40$ MPa with an initial modulus of elasticity of $E_0 = 40000$ MPa. Throughout this study it is assumed that sufficient bearing reinforcement is used to obtain the required loads and, hence, bearing failure is not the primary mode of failure. To obtain this numerically the elements directly beneath the loading plate, and one element to the side, to a depth w below the bearing surface were modelled with a peak confined concrete strength (f'_c'') of $f'_c'' = f'_c \times D/w \leq 2.5 f'_c$. The initial elastic modulus for the confined elements was kept at $E_0 = 40000$ MPa. The descending branch parameter used was $\gamma_2 = 5.0$ (refer Fig. 2b). The tension parameters used in this study were $\alpha_1 = 30$ and $\alpha_2 = 0.05$.

3.2. Constitutive relationships

The stress-strain relationship is expressed as

$$\sigma = \mathbf{D} \varepsilon \text{ or } d\sigma = \mathbf{D} d\varepsilon \quad (7)$$

where \mathbf{D} is the material elasticity matrix in the material coordinate system. To maintain symmetry in the constitutive relationships of uncracked concrete, Darwin and Pecknold (1977) proposed to let $\nu_2 E_1 = \nu_1 E_2 = \nu \sqrt{E_1 E_2}$ where E is the modulus of elasticity, ν is Poisson's ratio and the subscripts 1, 2 represent the materials principal axes. Therefore for plane stress

$$\mathbf{D} = \frac{1}{(1-\nu^2)} \begin{bmatrix} E_1 & \nu \sqrt{E_1 E_2} & 0 \\ \text{sym.} & E_2 & 0 \\ & & (1-\nu^2)G \end{bmatrix} \quad (8)$$

where G is the shear modulus of the uncracked concrete. The shear modulus used was that proposed by Darwin and Pecknold.

After cracking the Poisson's ratio effect is assumed to be eliminated, and the shear modulus is taken as a fraction of the cracking modulus, G_{cr} . The elasticity matrix is

$$\mathbf{D} = \begin{bmatrix} E_1 & 0 & 0 \\ \text{sym.} & E_2 & 0 \\ & & \beta G_{cr} \end{bmatrix} \quad (9)$$

In this study, β is taken as 0.7 at cracking ($\varepsilon = \varepsilon_{cr}$) and varies linearly to 0.3 at a strain of $10\varepsilon_{cr}$. For $\varepsilon > 10\varepsilon_{cr}$ $\beta = 3$. Previous experience has shown the FE model to be insensitive to the shear parameters selected.

4. Centrally loaded panels

Foster and Rogowsky (1997) undertook numerical studies on the behaviour of centrally loaded panels with a uniformly spaced reinforcement layout. Fig. 4 shows FE results of transverse stress distributions for linear, and non-linear analyses of a reinforced concrete panel having an area of transverse steel of $1500 \text{ mm}^2/\text{m}$ and a bearing plate width (w) to depth (D) ratio of $w/D = 0.2$. In the non-linear analysis, at the load for which the results were plotted, the concrete had undergone significant cracking and the maximum strain in the steel was $1100 \mu\varepsilon$ (approximately one half of its yield strain). It was shown that the behaviour of concrete panels is significantly different from the linear behaviour when cracking is considered, and when a uniform layout of transverse reinforcement is used. Fig. 4 indicates that the disturbed region extends beyond a distance of D from the bearing surface which can lead to lower quantities of bursting reinforcement.

Whilst the structure remains uncracked, the bursting stress distribution follows that of the linear analysis. When the tensile strength of the concrete is reached a substantial portion of the tensile force is transferred from the concrete to the steel reinforcement. For $w/D = 0.2$ (refer Fig. 4) the maximum bursting stress obtained from the non-linear analysis is approximately one half that of the linear analysis but extends well beyond the point where the linear peak starts to fall away. It must be kept in mind that in this analysis the post cracking residual concrete tensile strength has been set at a low value so as to distribute most of the tension force into the reinforcing steel. This low value would also represent residual concrete tensile

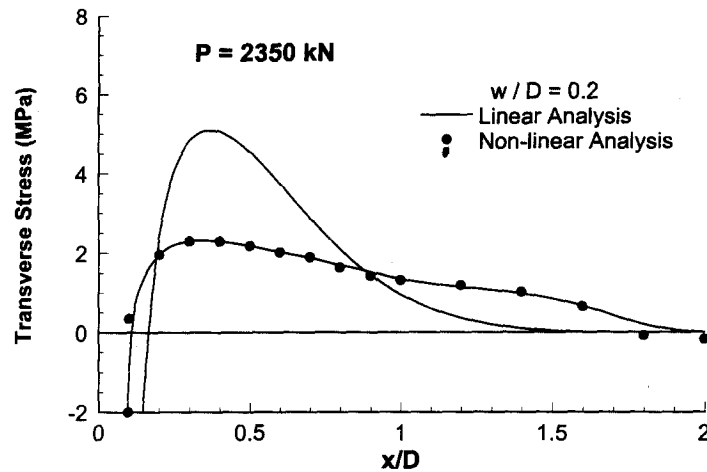


Fig. 4 Transverse stress distribution for a uniformly reinforced concrete panel with $w/D=0.2$.

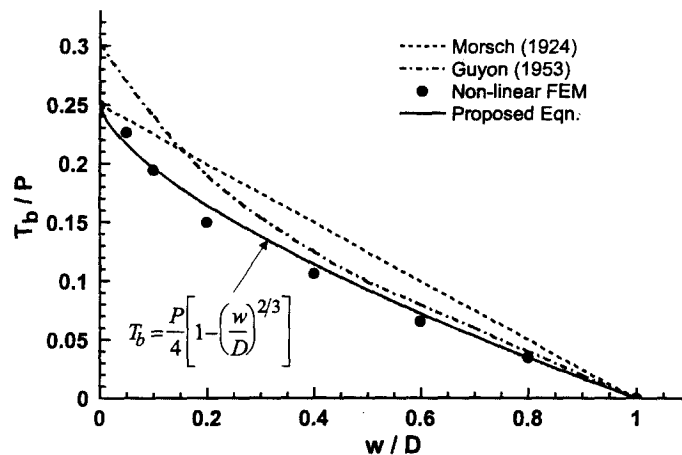


Fig. 5 Bursting forces for the serviceability limit state.

strength degradation that occurs under sustained loads or cyclic loads.

The total bursting forces expressed relative to the peak load for panels having various w/D are shown in Fig. 5, together with the curves of Guyon (1953) and Morsch (1924). The trend for the uniform mesh is similar to that predicted by Guyon but lies inside Guyon's curve. For the case of $w/D=0$ the bursting force computed is that predicted by Morsch. Foster and Rogowsky (1997) showed that the data generated by the non-linear FE analysis is described well with a simple modification to Morsch's equation; given as Eq. (10).

$$T_b = \frac{P}{4} \left[1 - \left(\frac{w}{D} \right)^{2/3} \right] \quad (10)$$

The FE mesh shown in Fig. 6 was used to model the behaviour at ultimate for w/D equal to 0.2 and 0.6. The meshes consisted of 75 eight-node membrane elements to model the concrete and 75 three-node bar elements to model the steel reinforcement. For the cases where the reinfor-

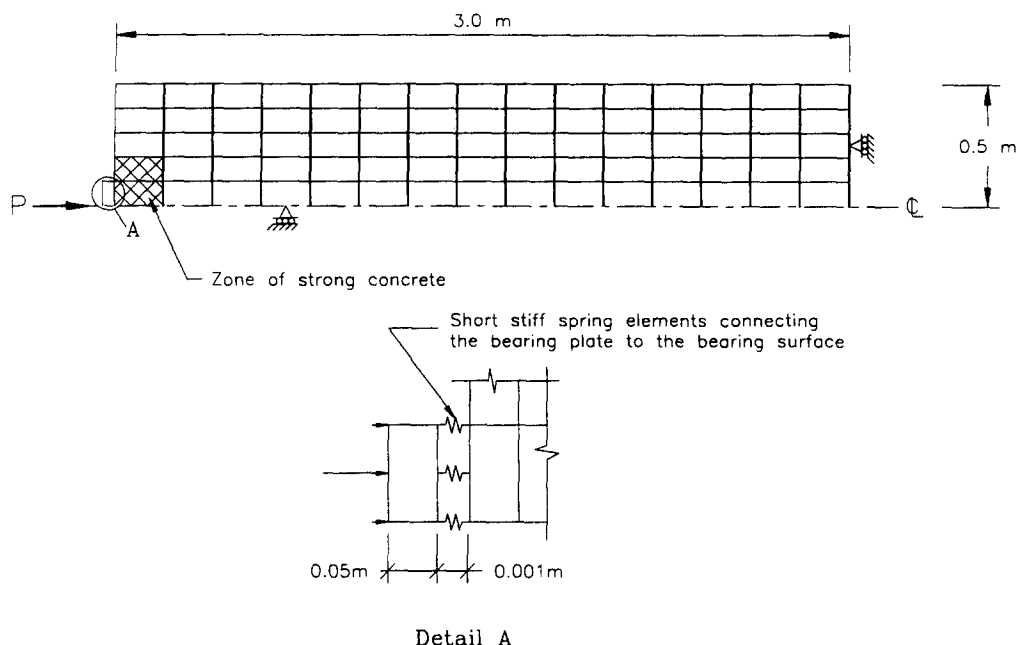


Fig. 6 FE mesh used in the strength limit state analyses for $w/D=0.2$.

cing steel was discontinued the additional bar elements were set with a low area and stiffness so as not to influence the analysis. To avoid any Poisson's effect between the bearing plate and the bearing surface the load was applied to the concrete bearing surface via short, stiff, spring elements (refer Fig. 6). The thickness of the panels was 150mm.

For the panels with $w/D=0.2$, the bursting forces were calculated for a design bearing load of 1700kN using Eq. (3), taking $d_c=w/4$. A uniform layout of reinforcement was used to carry the bursting forces calculated with the bars spaced at 200 mm centres. Details of the reinforcement layouts are given in Table 1. A similar analysis was undertaken for $w/D=0.6$ with a design load of 3000kN (refer Foster and Rogowsky 1997).

All panels reached their design load with the exception of the panel P02-20. In panel P02-20 the effective compressive strength of the concrete was diminished by the large transverse strains near ultimate. The development of transverse strains for panel P02-12 at various loads

Table 1 Reinforcement details for FE analyses with $w/D=0.2$, $P=1700$ kN

Panel	x_1/D^a	x_2/D^b	d_1/D	d_2/D	T_b (kN)	A_{st}^c (mm ²)
P02-04	0.2	0.4	0.1	0.5	680	1700
P02-08	0.2	0.8	0.1	0.9	380	950
P02-12	0.2	1.2	0.1	1.3	260	650
P02-16	0.2	1.6	0.1	1.7	200	500
P02-20	0.2	2.0	0.1	2.1	160	400

Notes a) x_1/D =location of first bar; b) x_2/D =location of last bar; c) A_{st} =total area of reinforcement; d) $D=1000$ mm

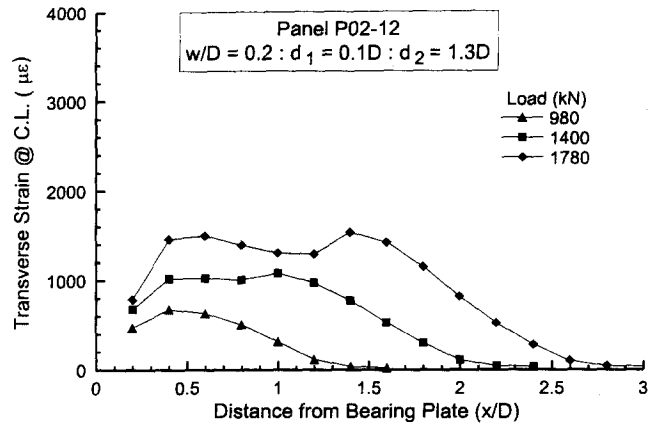


Fig. 7 Bursting strains versus distance from the bearing plate for panel P02-12.

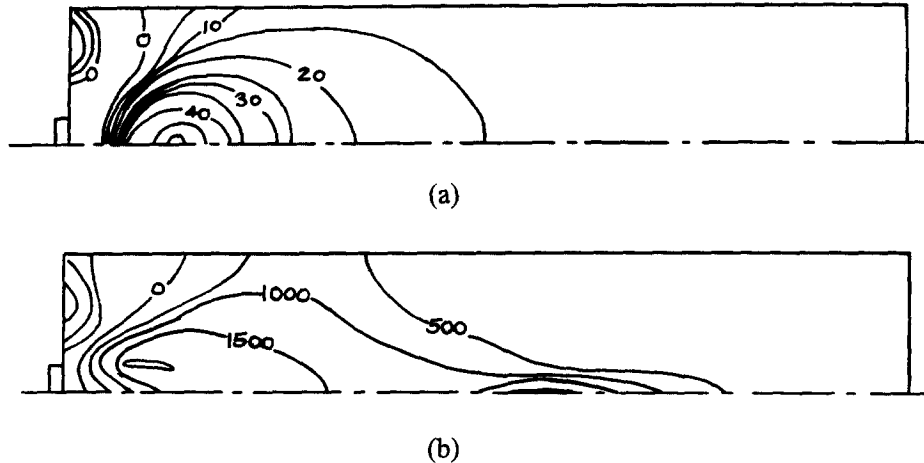


Fig. 8 Transverse strain contours (ϵ_{η}) for panel P02-12 at (a), $P=500$ kN, and (b) at $P=2200$ kN.

are shown in Fig. 7. At a load of 1400 kN the forces in the bursting steel are reasonably uniform, with a strain of approximately $1000 \mu\epsilon$. Also at this load, the strain in the concrete in the region immediately beyond the bursting steel is lower than the strains in the steel and thus the cracks are well controlled. With a strut and tie model, the selected reinforcement would give a service load of 850 kN (for a steel strain $1000 \mu\epsilon$) and an ultimate load of 1700 kN. It is reassuring to see the favourable comparison with the values given in Fig. 7. Fig. 8 compares the transverse strain contours through the panel before and after cracking where again the difference between linear and non-linear behaviour is clearly evident.

The optimum solution for a uniformly reinforced bursting region appears to be with the reinforcement continued to a distance of approximately $1.2D$ to $1.6D$ from the bearing plate. From a design perspective the reinforcing steel must satisfy both strength and serviceability requirements. For serviceability it is desirable for the steel reinforcement to remain elastic and to limit the maximum strain; typically to $1000 \mu\epsilon$ (equivalent to a stress of 200 MPa). The area of reinforcement calculated to satisfy Eq. (3) is required to be spread in proportion to the theoretical stress distribu-

tion.

For serviceability analyses, the simple strut and tie model represented by Eq. (3), and shown in Fig. 1, may be adopted. With this model and Eq. (4), the distance between the centroids of the bursting compression and bursting tension forces is

$$y_3 = \frac{D}{2} \left(\frac{1 - w/D}{1 - (w/D)^{2/3}} \right) \quad (11)$$

With $w/D=0$ in Eq. (11) the model given by Fig. 1 reverts to that proposed by Mörsch (1924). It can be shown that the results of the model are not highly sensitive to the depth of the bursting compression node, d_c . Thus any reasonable value may be selected. A value of

$$d_c = w/4 \leq D/10 \quad (12)$$

represents well the non-linear finite element results.

In the strength limit state the reinforcing steel yields and a wide range of reinforcing arrangements can be utilised. Assuming the bursting tension force is linearly distributed then the total bursting tension is again given by Eq. (3). For the strength limit state y_3/D may be taken arbitrarily within reasonable limits, say $1/2 \leq y_3/D \leq 3/4$. Some consideration should be given, however, to the effect of transverse strains on the compressive capacity of the concrete. Foster and Rogowsky (1997) show that as w/D was increased the optimum value for y_3/D also increased. Optimum being defined here as obtaining an almost uniform distribution of transverse strain at the design load. This is consistent with the serviceability model discussed above and, thus, Eq. (11) is appropriate for both the strength and serviceability limit states.

5. Eccentrically loaded panels

Similar design methods can be applied to members loaded away from the geometric centreline as for centrally loaded members. For the case of an eccentrically loaded panel, bursting forces may be calculated with the strut and tie model defined by Eq. (2) and with D_c substituted for D in Eq. (11).

To study the differences before and after cracking of an eccentrically loaded reinforced concrete panel, a FE analysis was undertaken for a one metre high by three metre long by 150 mm thick panel loaded at $e=D/6$. The FE mesh (shown in Fig. 9) consisted of 78 eight-node concrete elements and 30 three-node steel elements with the material properties given above. The design load was taken to be 3000kN and was applied through a 150mm bearing plate ($w/D=0.15$) giving a bursting force of 577kN (and requiring 1440mm² of transverse reinforcement). As for the previous analyses the load was applied via short, stiff spring elements to eliminate any Poisson's effects. The loading eccentricity of $e=D/6$ was chosen to produce zero strain in the bottom fibre of Bernoulli region. The bursting reinforcement was calculated using Eqs. (2) and (11), with D_c substituted for D to calculate y_3 .

Fig. 10 shows the results of the transverse stresses, measured along the loading line, at a load of $P=2730$ kN, for both linear and non-linear analyses. The non-linear stresses are calculated by distributing the force in the reinforcing steel over its local region and adding any residual tensile stress in the concrete. As for the centrally loaded panel, the peak transverse stresses obtained from the non-linear analysis are smaller than those for the linear analysis, but extends over

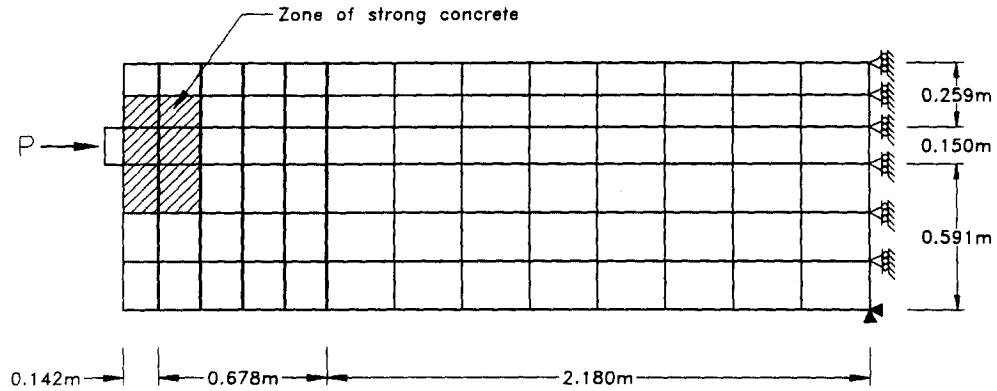


Fig. 9 FE mesh for eccentrically loaded panel with $e=D/6$ and $w/D=0.15$.

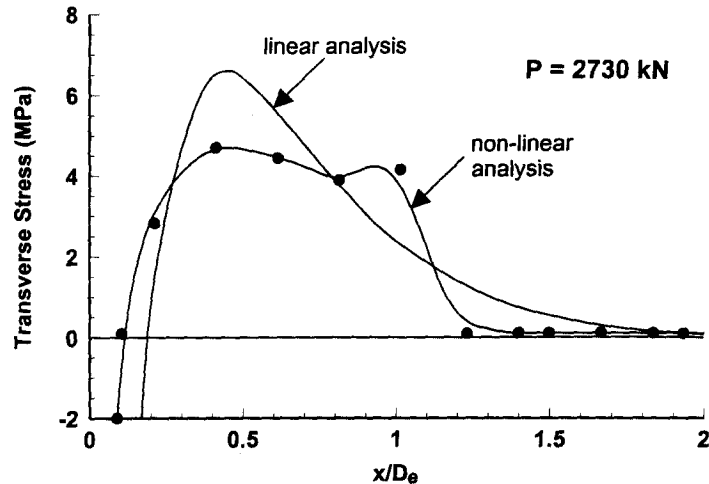


Fig. 10 Comparison between linear and non-linear analyses for an eccentrically loaded panel with $w/D=0.15$ and $e=D/6$.

a greater distance from the bearing surface. Fig. 11 shows transverse strain distributions before and after cracking. Before cracking the panel behaves in a linear manner with the disturbed zone penetrating approximately to a depth of approximately D into the panel. After cracking, significant force redistribution's occur and the disturbed zone moves further into the panel. Finally, at high load levels, high transverse strains occurred in the region immediately beyond the curtailment of the bursting steel (as was observed for the centrally loaded panels).

6. Conclusions

This study presented the results of finite element investigations into the behaviour of reinforced concrete panels loaded with a single concentrated force. Cases examined include centrally and eccentrically loaded panels. The results of the analyses showed a significant difference in the shape of the strain fields between linear and non-linear analyses (as shown in the before and

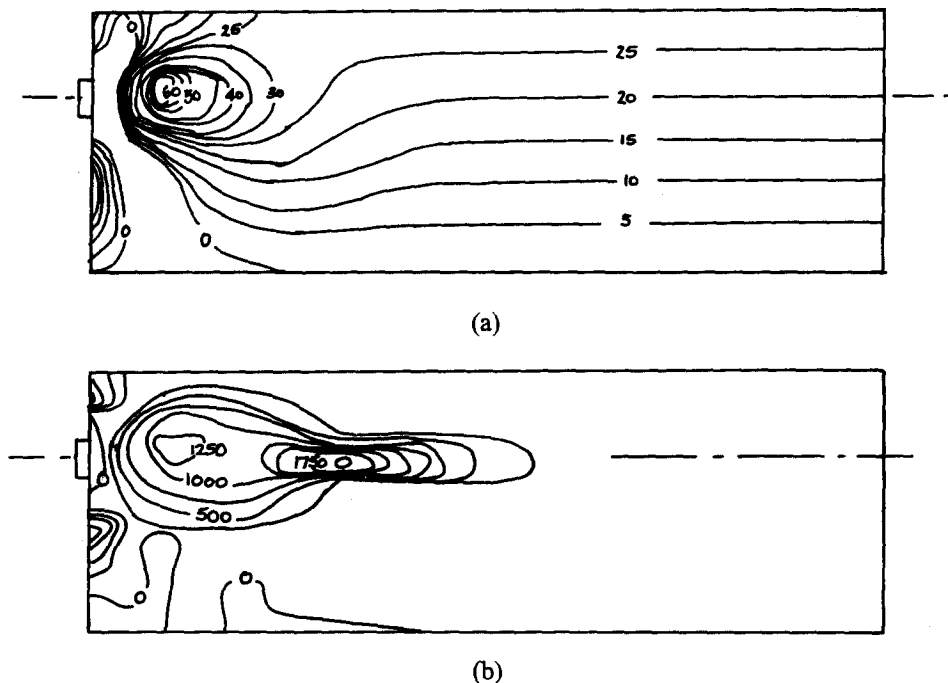


Fig. 11 Transverse strain contours (ϵ_{yy}) for a eccentrically loaded panel with $w/D=0.15$ at (a) $P=500$ kN, and (b) at $P=2200$ kN.

after cracking plots). One significant conclusion that comes from this study is that for materials exhibiting anisotropic behaviour, such as reinforced concrete in biaxial tension-compression, the depth of the disturbed region may extend significantly beyond a depth of D from the point of the disturbance. By taking advantage of this observation, the design engineer can move the centroid of the bursting force away from the bearing surface giving a smaller overall quantity of reinforcing steel, larger spacings between reinforcing bars and an improved transverse strain field. The final observation drawn from this research is that at least minimum reinforcement needs to be continued beyond the bursting zone ensure cracking does not get out of control in the strength limit state.

References

- Darwin D. (1977), and Pecknold D.A. "Nonlinear biaxial stress-strain law for concrete", *Journal of the Engineering Mechanics Division, ASCE*, **103**(EM2), Apr., 229-241.
- Foster, S.J. (1992a), "The structural behaviour of reinforced concrete deep beams", *PhD. Dissertation*, School of Civil Engineering, University of New South Wales, Sydney, Australia, August.
- Foster, S.J. (1992b), "An application of the arc length method involving concrete cracking", *Int. J. Num. Meth. Eng.*, **33**(2), 269-285.
- Foster, S.J., Budiono, B., and Gilbert R.I. (1996), "Rotating crack finite element model for reinforced concrete structures", *Computers & Structures*, **58**(1), 43-50.
- Foster S.J., and Rogowsky, D.M. (1996), "Design of concrete panels subject to bursting tension forces resulting from in-plane concentrated loads", *UNICIV Report*, R-347, School of Civil Engineering.

- University of New South Wales, Kensington, 47pp.
- Foster S.J., and Rogowsky, D.M. (1997), "Bursting forces in concrete panels resulting from in-plane concentrated loads", *Magazine for Concrete Research*, (in press).
- Guyon, Y. (1953), *Prestressed Concrete*, F.J. Parsons, London.
- Mörsch, E. (1924), "Über die berechnung der gelenkquader", *Beton und Eisen* **23**(12), 156-161.
- Rogowsky, D.M. and MacGregor, J.G. (1983), "Shear strength of deep reinforced concrete continuous beams", *Structural Eng. Report*, 110, Dept. of Civil Engineering, University of Alberta, Edmonton, Alberta, Canada, Nov., 178pp.
- Saenz L.P. (1964), "Discussion of equation for the stress-strain curve for concrete", by Desayi and Krishnan. *ACI Journal, Proceedings*, **61**(9), 1229-1235.
- Vecchio F.J. and Collins M.P. (1986), "The modified compression field theory for reinforced concrete elements subjected to shear", *ACI Journal Proceedings*, **83**(22), 219-231.